Automatic Building Reconstruction from Cadastral Maps and Aerial Images

Franck Taillandier
Institut Géographique National - laboratoire MATIS, 2-4 avenue Pasteur, 94165 Saint-Mandé
franck.taillandier@ign.fr

Commission III, WG III/4

KEY WORDS: Building, Reconstruction, Modeling, Aerial, Image, Automation, Systems, Photogrammetry, Cadastral maps.

ABSTRACT:

The approach described in this paper is intended for 3D building reconstruction on large and dense urban areas. It provides a real-time solution for automatic inferring of polyhedral rooftops of buildings from cadastral maps and aerial images. From the initial planimetric outline and hypotheses of planes inferred from it, a set of rooftop models depending on two parameters (slope and gutter altitude) is extracted through maximal cliques enumeration methodology. Among this family, the best representation is chosen by centered correlation on Digital Elevation Model computed by correlation from aerial images. Finally, slope and altitude are determined by L1 minimization. Some results on real data show the validity of the algorithm that favors robustness against generality and is designed for integration in a semi-automatic platform for 3D urban databases constitution.

1. INTRODUCTION

1.1 Context

3D databases constitution of urban areas becomes more and more important in many fields such as virtual tourism, fighting simulations or urban environment planning. Although manual techniques are available, costs and time for their constitution remain crippling for large and dense urban areas. A lot of actual research tend therefore towards automated solutions.
The main issue of these automatic systems is to provide an "acceptable caricature" of buildings. Although the system should remain very generic to handle the tremendous complexity of roof structures in dense urban areas, some simplifications of shapes may indeed be acceptable: simplifications concerning dormer windows, chimneys or building recesses can be tolerated according to some specifications. Despite promising results, most of automatic approaches for building reconstruction from aerial images or laser scanning data fail to handle dense urban areas and can only deal with suburban areas. Obviously, automatic solutions have to face the complexity and the diversity of roof structures present in urban areas and the presence of occlusions such as vegetation. Furthermore, they need to overcome errors of primitives detectors: under- or over-segmentation and geometric inaccuracy. These difficulties led to the increasing use of cadastral or map limits often available in industrial countries and that supply the planimetric outlines of buildings, essential to facilitate the 3D reconstruction. Our method takes place in this context. The goal is to provide an automatic method for 3D reconstruction from cadastral maps and aerial images. Our algorithm should take place in a semi-automatic platform where the operator can select the building to reconstruct and edit, when necessary, its 2D outline but 3D reconstruction is then automatically performed. Therefore we focus on supplying a real-time automatic technique without throwing the planimetric outline back into question.

1.2 State of the Art

Most automated systems for buildings reconstruction from solely aerial images can be classified as data-based or model-based. In the former one, authors (Baillard and al., 1999; Heuel and al., 2000; Ameri and Fritsch, 2000; Scholze and al., 2002) have chosen not to restrict the set of available shapes for roof structures. They often use only one kind of primitives (3D segments for (Baillard and al., 1999; Scholze and al., 2002), corners in (Heuel and al., 2000) and planar patches in (Ameri and Fritsch, 2000)) and handle under-segmentation or primitives errors with difficulty. On the contrary, the latter ones (Fuchs and Le-Men, 1999; Fischer and al., 1998) use some models of buildings to restrict the set of possible shapes. This external knowledge enables to overcome lack of detection and over detection. They both provide promising results but, despite obvious efforts, are still limited to very simple forms and thus can not handle all the shapes available in urban or suburban areas. All these methods have shown their limits in dense urban areas and fail to overcome most of the difficulties encountered in these areas.

In another context, with cadastral limits, (Jibrini, 2002; Flamanc and al., 2003; Vosselman and Suveg, 2001; Brenner and al., 2001) have proposed interesting approaches. (Jibrini, 2002) searches, from a set of planes for the best continuous polyhedral surface enclosed in the cadastral limits. This very generic modeling handles over-detection of planes but is limited due on the one hand to combinatorial consideration for the exploration of possible building models and on the other hand to over-segmentation or errors of planes hypotheses through Hough Transform. (Vosselman and Suveg, 2001) segment the ground plans and detect roof faces through, once again, Hough Transform method thus facing the same problems as the previously cited method. (Flamanc and al., 2003; Brenner and al., 2001) use methods related to the straight skeleton to derive likely hypotheses of buildings. Some topological problems may arise and these methods are difficult to generalize. Our strategy comes from the very general method described in (Taillandier and Deriche, 2004). This method inherits from (Jibrini, 2002) but ensures more robustness for plane extraction and reduces the set of shapes to more likely models of buildings.

1.3 General Scheme

In this paper, we focus on a method for 3D building reconstruction from cadastral maps and aerial images (figure 1). We will assume a good planimetric delineation of cadastral outline and we will look to meet real-time requirements. Robustness will be favored against generality. As stated previously, the possibility to supply an "acceptable caricature" enables to tolerate some simplifications and thus to accept shape close but not exactly conform to reality. This justifies therefore this choice and leads to restrict the family of models of buildings to a classical set of buildings. In this article, we focus on a reduced family that depend only on the cadastral outline and two additional parameters: slope and gutter altitude.

In a first step, the algorithm infers one *simulation* plane for each segment of the cadastral outline. From the intersection of all planes, a 3D graph is deduced in which all possible models of buildings are enumerated through maximal cliques techniques. After a pruning step, a family of *likely models* is available in which the choice of the best representation is made through centered correlation on a Digital Elevation Model (DEM) obtained by correlation from images. The last step consists of determining some parameters to fit the model on this correlation DEM.

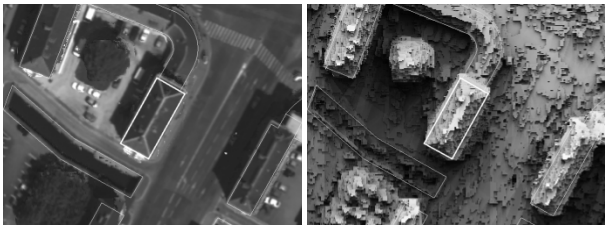

Figure 1: Focusing zone with cadastral outline, either on an orthophotography or on a correlation DEM.

2. MODELS ENUMERATION

2.1 Planes Inferring

As stated previously, most of automatic approaches fail to give a good reconstruction because of poor accuracy of the initial primitives. Most systems rely indeed on DEM segmentation for plane estimation. However, most of DEM are corrupted by erroneous points, either due to correlation failure or to superstructures of roofs such as dormer windows or chimneys. To avoid these artefacts, in our case, planes are directly deduced from the cadastral outline, without any segmentation step, thus reducing the risk of errors.

The cadastral outline is assumed to correspond to horizontal gutters with an arbitrary altitude $z_g = 0$. For each segment of gutter, one plane is inferred (figure 2). Going through the segment and orthogonal to it, its slope α is also arbitrarily fixed at 45° ($\tan\alpha = p = 1$). The two parameters z_g and p will be defined at the end of the process by fitting the final model on correlation DEM.

This modeling is well suited for buildings with symmetrical roofs with central ridge, very common in European countries but it can be also used for non horizontal flat roof as it will be shown afterwards.

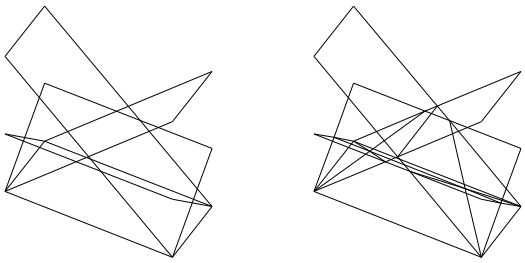

Figure 2: Inferred planes (left) and plane arrangement or 3D graph (right) deduced from the intersection of all plane hypotheses in the previous example.

2.2 Exhaustive Search

The process follows the scheme described in (Taillandier and Deriche, 2004), which is an extension of (Jibrini, 2002). It consists in enumerating, from the hypotheses of planes, all possible roof structures, meeting a very general definition of building rooftops. A roof is indeed defined as a polyhedral structure *with no overhang* covering the cadastral outline. This definition enables to model most of rooftops seen from aerial data.

To achieve this enumeration, all hypotheses of planes are intersected, leading to a plane arrangement that builds up a 3D graph of facets $\mathcal{G}$ (see figure 2 and schematic example on a cross-section in figure 3(a)). This graph is enclosed in a prismatic volume whose base is the cadastral outline. In this graph, all facets are oriented with their normals pointing upward. Two adjacent facets are *coherent* along their common edge $\mathbf{s}$ if, with the notations of figure 4(a):

$$[\mathbf{s}, \mathbf{v_1}, \mathbf{n_1}].[\mathbf{s}, \mathbf{v_2}, \mathbf{n_2}] < 0 \qquad (1)$$

where $[\mathbf{a}, \mathbf{b}, \mathbf{c}]$ stands for the triple scalar product. Intuitively, two facets are coherent if, assuming the normal points towards the "exterior" of a volume, the normal direction remains coherent when switching from one facet to the other one. Figure 4 shows some counterexamples.

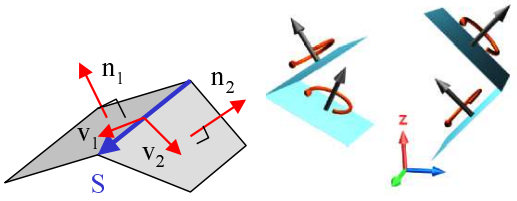

(a) two coherent facets (b) some non coherent facets

Figure 4: facets coherence.

An edge in this graph is said to be locally admissible if either it projects exactly on a segment of the cadastral outline either there are at least two facets coherent along it (there is thus at least one facet on *each* side of the edge). A facet is *locally admissible* if it is locally admissible along its bordering edges. An *admissible surface* is a continuous polyhedral surface made of coherent facets, whose horizontal projection completely covers the whole cadastral planimetric surface.

From (Taillandier and Deriche, 2004), it can also be shown that, given our context and especially normals orientations (normals pointing upwards), an admissible surface is a continuous polyhedral surface *with no overhang*. Thus, in this case, the search for roof models *boils down* to the search for all possible admissible surface. Before this search, which is a NP-hard problem, in the 3D graph, facets that can not belong to any admissible surface are recursively suppressed (these are facets hanging on top and bottom parts of the virtual prismatic volume).

The enumeration of roof models is then performed through maximal cliques method in a so-called compatibility graph. Two facets are (not) compatible if they (do not) belong to at least one common admissible surface. (Jibrini, 2002) and (Taillandier and Deriche, 2004) describe an algorithm to compute for each facet the set of its compatible facets. At the end of this computation, one can derive an uncompatibility graph $\bar{\mathcal{G}}_c$ in which each node is a facet of $\mathcal{G}$ and each arc links two non compatible facets (figure 3(b)). $\bar{\mathcal{G}}_c$ is the graph complement of the compatibility graph graph $\mathcal{G}_c$. As in (Jibrini, 2002), *the admissible surfaces of* $\mathcal{G}$ *are*

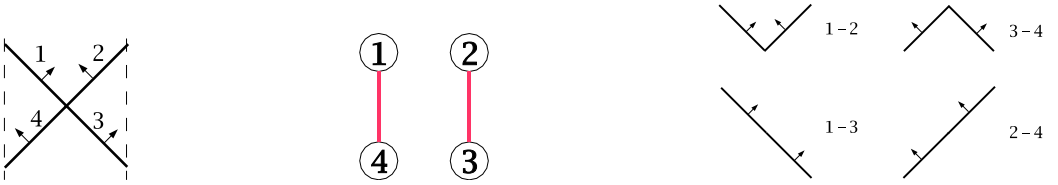

(a) 3D Graph with numbered and oriented facets

(b) uncompatibility graph $\bar{\mathcal{G}}_c$

(c) models deduced from exhaustive search presented as admissible surface or maximal independent set

Figure 3: 3D graph (a), uncompatibility graph (b) and models of rooftops (c) on a cross-section example. Two planes are detected leading to a 4-facet 3D graph (or plane arrangement) as presented in figure a. The dashed lines symbolize the cadastral facades as seen in this 2D schematic example. The upper left model in the solutions shall be removed in the pruning steps.

the maximal cliques of $\mathcal{G}_c$ or in an equivalent way, *the admissible surfaces of* $\mathcal{G}$ *are the maximal independent sets of* $\bar{\mathcal{G}}_c$. We recall that a clique is a set of nodes of a graph that are all pairwise connected. A maximal clique defines a clique for which no node can be added while keeping this property. Conversely, an independent set is a set of nodes such that for any pair of nodes, there is no edge between them. It is maximal if no more node can be added and it still be an independent set. The equivalence between admissible surfaces and maximal cliques is proved in (Taillandier and Deriche, 2004).

The search for admissible surfaces and consequently for roof models thus boils down to a search for maximal cliques, which is unfortunately a NP-hard problem. One can however find efficient algorithms to solve for these solutions (Bron and Kerbosch, 1973) and enable a deep study in our peculiar graphs (see figures 5 and 3(c) for a schematic example).

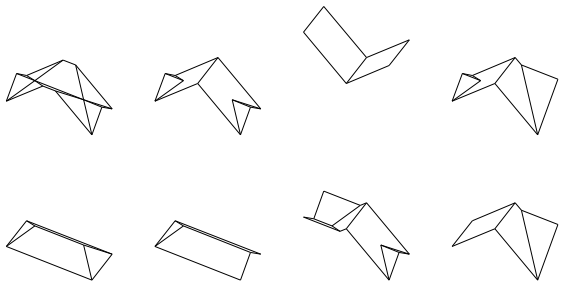

Figure 5: Some of the 83 solutions for the example of figure 1 before pruning steps.

2.3 Models Pruning

The previous section describes a procedure to enumerate any kind of polyhedral surface with no overhang covering the whole cadastral surface. However, this set of roof structures is vast and is made of some structures not likely to represent a building roof. Therefore, it needs to be pruned to supply a restricted family of buildings.

The first step of pruning is geometrical and consists of pruning all roof models for which at least one face has a area of less than 1m^2 or for which two edges make an angle of less than 10°. These conditions are weak enough to remove erroneous models without altering the generality of the approach.

The second step of pruning consists of two different procedures. In the first one, each model with a face not hanging on one of the facades defined by the cadastral outline is removed. In the last one, each model, for which at least one face does not touch the gutter segment from which the plane it lies one has been inferred, is removed. Globally, these pruning steps enables to cut down the first set of models to a considerably reduced family of models, which depend on the cadastral outline and only two parameters: slope (p) and altitude of gutter (z_g). As a matter of fact, generality is not preserved but robustness has been favored in our context. As it can be seen in figure 6, a lot of models can still be represented, including one-face building.

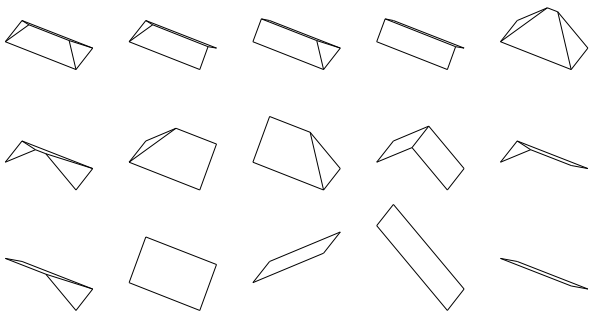

Figure 6: All the 15 solutions in Γ after pruning, sorted by correlation score.

3. Model Selection and Parameters Estimation

3.1 Correlation Criteria

The previous section describes the way of enumerating a set of likely models of buildings Γ. The main difficulty in the choice of the final representation comes from the fact that all planes are inferred with 2 arbitrarily fixed parameters. Models of Γ are simulation models and are not (yet) in accordance with reality !

To overcome this difficulty, one uses centered correlation on DEM. The following explains how this method enables to get rid of this issue. For each point $\mathbf{u}(u, v)$ of the correlation DEM inside the cadastral outline, an unique synthetic altitude can be computed for each admissible surface. From the property of admissible surface, this 2D point vertically projects indeed on one and only one face of the model M. This face lies on a plane inferred from a cadastral segment. The horizontal distance between $\mathbf{u}$ and this cadastral segment is trivial to compute and will be noted $d_M(u, v)$. For the model M, the synthetic altitude of $\mathbf{u}(u, v)$ is thus:

$$z_M(u, v) = z_g + p.d_M(u, v) \quad (2)$$

For each model of building M, a synthetic DEM S_M can thus be computed with the values initially fixed for the parameters p and z_g as given in section 2.1. The values of S_M are defined uniquely inside the cadastral outline.

As shown in figure 7, a centered correlation is then performed between S_M and the DEM obtained by correlation from aerial images C (Baillard and Dissard, 2000). For each point (u, v) of S_M, centered correlation on a correlation window of (2v+1)x(2v+1) pixels is performed with the corresponding point in C as recalled in equation 3. In practice, we have chosen a 3x3 correlation window ($v = 1$). The correlation score is thus given for each pixel of S_m by the classical relation:

$$c_M(u,v) = \frac{\sum_{i=-v}^{i=+v}\sum_{j=-v}^{j=+v} \bar{S}_M(u+i,v+j)\bar{C}(u+i,v+j)}{N(u,v)} \quad (3)$$

where

$$\bar{S}_M(u,v) = S_M(u,v) - \frac{1}{(2v+1)^2}\sum_{i=-v}^{i=+v}\sum_{j=-v}^{j=+v} S_M(u+i,v+j) \quad (4)$$

$$\bar{C}(u,v) = C(u,v) - \frac{1}{(2v+1)^2}\sum_{i=-v}^{i=+v}\sum_{j=-v}^{j=+v} C(u+i,v+j) \quad (5)$$

and

$$N(u,v) = \sqrt{\sum\sum\left(\bar{S}_M(u+i,v+j)\right)^2 \sum\sum\left(\bar{C}(u+i,v+j)\right)^2} \quad (6)$$

The sum of correlation scores of all points of S_M enclosed in the cadastral outline gives a global score v_M for each model of Γ as shown in equation 7.

$$v_M = \sum_{(u,v)\in S_M} c_M(u,v) \quad (7)$$

The model $\hat{M}$ that maximizes this global score v_M is chosen as the best representation. Some weight could be introduced to balance this data adequation term and some model complexity term as in (Taillandier and Deriche, 2004). However, previous pruning steps are supposed to have restricted Γ to likely building models among which no one should be favored.

This approach enables to avoid altitude dependency and thus overcome the non determination of z because the correlation is *centered*. The dependency with p still exists but is reduced. With no concurrent slopes for each plane inferred from one gutter segment and given the pruning steps, this criteria reveals robust enough. A roof face with a slope opposite to the reality will indeed have a lower correlation score than when the slope has the same orientation. This method focuses consequently on slope orientation with less incidence due to the parameter p.

Let us note that correlation sum can be pre-computed on each facet in the 3D graph, which drastically reduces the time needed for score evaluation for each model. For each model M, the computation indeed boils down to a sum on the facets making up M. This optimization enables to ensure real-time goal for the global application.

3.2 Slope and Altitude Estimation

As stated previously, z_g and p are to be determined. They are computed by minimization on the correlation DEM. The last section recalled how to compute an altitude for each point of each model, depending on z_g and p. For $\hat{M}$, one looks for z_g and p that minimize

$$\begin{aligned}\mathcal{Q}(z_g,p) &= \sum_{(u,v)\in S_{\hat{M}}} |C(u,v) - S_{\hat{M}}(u,v)| \\ &= \sum_{(u,v)\in S_{\hat{M}}} |C(u,v) - (z_g + p.d_{\hat{M}}(u,v))|\end{aligned} \quad (8)$$

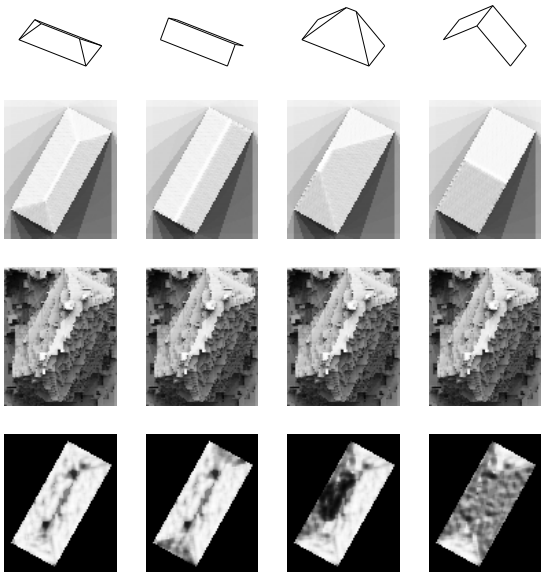

Figure 7: First row: initial 3D models. Second row: synthetic DEM obtained from the model. Third row: initial correlation DEM. Fourth row: correlation score for each pixel of the synthetic DEM with grayscale colors (brighter colors referring to high correlation scores).

L1 minimization has been favored because of its robustness. This robustness is necessary to overcome correlation errors in the correlation DEM C. It is also useful for roof superstructures such as dormer windows or chimneys that are not to be modeled in this application. They give indeed high correlation in C scores and can alter parameters estimation with Least Square Estimation.

Figure 8: Result on the example after parameters determination.

4. Results and Conclusion

4.1 Results

Figures 8, 9 and 10 show some results. All results have been obtained in real time or quasi real-time, meaning a delay of less than 1 second (real-time) or 5 seconds (quasi real-time) for a building to be modeled. Very complex buildings rooftops can be modeled through this approach.

More quantitatively, on 600 selected cadastral outlines, a visual inspection showed that more than 90% give a correct reconstruc-

tion with this approach, meaning the reconstructed shape is true to reality except for the tolerated omissions of small details such as chimneys or dormer windows. The algorithm supplies more robustness than generality and shows a good behavior for the description of symmetric buildings with central ridge. Main failures are due to buildings that can not be described through this modeling (mainly dissymetric rooftops or horizontal flat rooftops).
As far as geometric accuracy is concerned, the global Root Mean Square (RMS) for altitude on more than 1.2 million of points with regard to the correlation DEM is 68cm with a 25cm ground pixel and altimetric accuracy of 60cm for this correlation DEM.

Figure 9: Results on the center of the city of Amiens in France.

4.2 Discussion

Obviously, the actual algorithm has lost the generality of the initial work. once again, in this case, robustness is favored but some work is under progress to increase generality while still meeting the requirements of robustness and real-time needed for operational software environment. The very general framework presented in (Taillandier and Deriche, 2004) makes this process a lot easier. The algorithm should also be able to account for horizontal flat rooftops. In the actual version, because of correlation process, theoretically, these roofs can indeed not be modeled. A preprocessing step relying on small altitude variance could get rid of this drawback.

Another limitation of the actual method is its inability to account for cadastral planimetric errors. In this case facades hypotheses have to be inferred and introduced in the algorithm as in (Taillandier and Deriche, 2004).

In semi-automatic environment, the main limitation lies in the absence of alert protocol so as to focus the operator on zones where the algorithm produces incorrect reconstructions. This alert criteria could be a high RMS on correlation DEM.

4.3 Conclusion

We have presented an algorithm for 3D reconstruction of roof structures of buildings from cadastral ground maps and aerial images. Aiming at dense and large urban areas, this algorithm shows good capabilities and results are promising for massive production in these areas while still meeting real-time requirements necessary for semi-automatic platform. The general framework underlying the process presented in this article should also enable to quickly improve the generality of the approach while maintaining a high rate of good 3D reconstructions.

REFERENCES

Ameri, B. and Fritsch, D., 2000. Automatic 3D building reconstruction using plane-roof structures. In *ASPRS*, Washington DC.

Baillard, C. and Dissard, O., 2000. A stereo matching algorithm for urban digital elevation models. *Photogrammetric Engineering and Remote Sensing*, 66(9):1119–1128.

Baillard, C., Schmid, C., Zisserman, A., and Fitzgibbon, A., 1999. Automatic line matching and 3D reconstruction of buildings from multiple views. In *Proceedings of ISPRS Conference on Automatic Extraction of GIS Objects from Digital Imagery, IAPRS*, volume 32(3), pages 69–80.

Brenner, C., Haala, N., and Fritsch, D., 2001. Towards fully automated 3d city model generation. In Baltsavias, E., Gruen, A., and Gool, L., editors, *Automatic Extraction of Man-Made Objects from Aerial and Space Images (III)*, pages 47–57, Centro Stefano Franscini, Monte Verit, Ascona. A.A. Balkema Publishers.

Bron, C. and Kerbosch, J., 1973. Algorithm 457: Finding all cliques of an undirected graph. *Communications of the ACM*, 16(9):575–577. ISSN:0001-0782.

Fischer, A., Kolbe, T., Lang, F., Cremers, A., Förstner, W., Plümer, L., and Steinhage, V., 1998. Extracting buildings from aerial images using hierarchical aggregation in 2D and 3D. *Computer Vision and Image Understanding*, 72(2):163–185.

Flamanc, D., Maillet, G., and Jibrini, H., 2003. 3d city models: an operational approach using aerial images and cadastral maps. In Ebner, H., Heipke, C., Mayer, H., and Pakzad, K., editors, *Proceedings of the ISPRS Conference Photogrammetric on Image Analysis (PIA'03)*, volume 34 of *The International Archives of the Photogrammetry, Remote Sensing and Spatial Information Sciences*, pages 53–58, Münich, Germany. Institute for Photogrammetry and GeoInformation University of Hannover, Germany. ISSN: 1682-1750.

Fuchs, F. and Le-Men, H., 1999. Building reconstruction on aerial images through multi-primitive graph matching. In Kropatsch, W. and Jolion, J.-M., editors, *Proceedings of the 2nd IAPR-TC-15 Workshop on Graph-based Representations*, pages 21–30, Vienna, Austria. Österreiche Computer Gesellschaft.

Heuel, S., Lang, F., and Frstner, W., 2000. Topological and geometrical reasoning in 3D grouping for reconstructing polyhedral surfaces. In *Proceedings of the XIXth ISPRS Congress*, volume 33 of *The International Archives of the Photogrammetry, Remote Sensing and Spatial Information Sciences*, pages 397–404, Amsterdam. ISPRS.

Jibrini, H., 2002. *Reconstruction automatique des bâtiments en modèles polyèdriques 3D à partir de données cadastrales vectorisées 2D et d'un couple d'images aériennes à haute résolution.* Thèse de doctorat, Ecole Nationale Supérieure des Télécommunications, Paris.

Scholze, S., Moons, T., and Van-Gool, L., 2002. A probabilistic approach to building roof reconstruction using semantic labelling. In Gool, L. J. V., editor, *Proceedings of the 24th DAGM Symposium*, volume 2449 of *Lecture Notes in Computer Science*, pages 257–264, Zürich, Switzerland. Springer.

Taillandier, F. and Deriche, R., 2004. Automatic buildings reconstruction from aerial images: a generic bayesian framework. In *Proceedings of the XXth ISPRS Congress*, The International Archives of the Photogrammetry, Remote Sensing and Spatial Information Sciences, Istanbul, Turkey. ISPRS.

Vosselman, G. and Suveg, I., 2001. Map based building reconstruction from laser data and images. In Baltsavias, E., Gruen, A., and Gool, L., editors, *Automatic Extraction of Man-Made Objects from Aerial and Space Images (III)*, pages 231–239, Centro Stefano Franscini, Monte Verit, Ascona. A.A. Balkema Publishers.

Figure 10: 3D view of results on the center of the city of Amiens in France.